

**DISCOVERY OF MULTI-TARGETING
INHIBITORS IN PARKINSON'S DISEASE USING
MOLECULAR MODELLING, *IN SILICO* ADMET
PROFILING, AND BEHAVIOURAL ANALYSIS
OF ZEBRAFISH LARVAE**

SANI NAJIB YAHAYA

UNIVERSITI SAINS MALAYSIA

2025

**DISCOVERY OF MULTI-TARGETING
INHIBITORS IN PARKINSON'S DISEASE USING
MOLECULAR MODELLING, *IN SILICO* ADMET
PROFILING, AND BEHAVIOURAL ANALYSIS
OF ZEBRAFISH LARVAE**

by

SANI NAJIB YAHAYA

**Thesis submitted in fulfilment of the requirements
for the degree of
Doctor of Philosophy**

February 2025

ACKNOWLEDGEMENT

I would like to express my profound gratitude to ALLAH SWT for giving us opportunity, health, guide, and help us endlessly in finishing this thesis writing. I thank ALLAH for his abundant grace and mercy upon me to complete this course of study. I would like to specifically thank Bayero University Kano for finding me worthy of nomination to study this program. I would like to graciously thank my supervisor in person of Prof. Dr. Mohd Nizam Bn Mordi for all the support, immense guidance, assistance, comments, and fatherly advice during this study as well as providing materials and equipment for this research. My special thanks go to Dr. Yusuf Oloruntoyin Ayipo, Waleed Abdullah Ahmad Alananzeh, and Muhammad Saifuddin for their passionate understanding, guidance, and support. Many thanks to staff and students of Centre for Drug Research (CDR) especially, the Journal Club members for words of encouragement and assistance throughout the program. Friends you deserve a great and warm thanks especially, Dr Sha'aban Abubakar, Dr. Ibrahim Jatau, Mustapah Abubakar, and Dr Mustapaha Mohammed. I would like to send my special thanks to the sponsor of the programme the Tertiary Education Trust Fund (TETFUND). All this work would not have been feasible and possible without the blessings, guidance, love, and care from my beloved parents Alhaji Yahaya Sani and Hajiya Binta Mahmud. Indeed, I remain indebted to my loving, supportive, caring, encouraging, and beautiful family, specifically my wife Rabi'atu Aliyu Najib, my daughter (Aisha), and Son (Aliyu), for their sacrifice and patience towards the struggle.

TABLE OF CONTENTS

ACKNOWLEDGEMENT	ii
TABLE OF CONTENTS	iii
LIST OF TABLES	xiv
LIST OF FIGURES	xvii
LIST OF SYMBOLS	xxv
LIST OF ABBREVIATIONS	xxvi
LIST OF APPENDICES	xxxii
ABSTRAK	xxxiii
ABSTRACT	xxxv
CHAPTER 1 INTRODUCTION	1
1.1 Background	1
1.2 Problem Statement	6
1.3 General Objective	7
1.4 Specific Objectives of the study.....	7
1.5 Flow chart of the research.....	9
CHAPTER 2 LITERATURE REVIEW	10
2.1 Parkinson's Disease (PD).....	10
2.1.1 Symptoms of PD	10
2.1.2 α -synuclein (α -syn)	13
2.1.2(a) α -syn's structural characteristics	14
2.1.2(b) Role and function of α -syn	17
2.1.2(c) Structural alterations of α -syn.....	19
2.1.2(c)(i) Aggregation and propagation	19
2.1.2(c)(ii) Misfolding of α -syn	20

2.1.2(c)(iii)	Phosphorylation and toxicity of α -syn.....	20
2.1.2(d)	Therapeutic alternatives inhibitory compounds of α -syn	22
2.1.3	Human tau protein.....	27
2.1.3(a)	Phosphorylation of tau protein.....	28
2.1.3(b)	Tau protein and parkinsonism.....	28
2.1.4	Prolyl oligopeptidase (POP) enzyme	30
2.1.4(a)	Prolyl Oligopeptidase (POP) enzyme and Parkinson's Disease (PD)	32
2.1.5	α -syn oligomers, toxicity, and Parkinson's Disease (PD).....	34
2.2	Diagnosis of Parkinson's Disease (PD)	38
2.3	Pharmacological management of Parkinson's Disease (PD).....	38
2.3.1	Classes of drugs for Parkinson's Disease (PD) management	38
2.3.1(a)	Dopamine agonist	39
2.3.1(b)	Monoamine Oxidase B inhibitors (MOBI).....	41
2.3.1(c)	Catechol-O-methyltransferase (COMT) inhibitors	43
2.3.1(d)	Other classes of anti-Parkinson's Disease (PD) inhibitors drugs	45
2.3.1(d)(i)	Selective serotonin re-uptake inhibitors (SSRIs)	45
2.3.1(d)(ii)	Acetylcholine inhibitors	47
2.3.1(d)(iii)	Tricyclic antidepressants	49
2.3.1(d)(iv)	Amantadine.....	49
2.3.2	Natural compounds as source for anti-Parkinson's Disease (PD).....	50
2.4	Modelling of Parkinson's Disease (PD).....	52
2.4.1	<i>In vitro</i> and cell culture modelling of Parkinson's Disease (PD).....	53
2.4.2	<i>In vivo</i> modelling of Parkinson's Disease (PD).....	53

2.4.2(a)	1-methyl-4-phenyl-1,2,3,6-tetrahydropyridine (MPTP)	54
2.4.2(b)	6-hydroxydopamine (6-OHDA)	54
2.4.2(c)	Rotenone	55
2.4.2(d)	Paraquat	56
2.4.3	Animals as model for Parkinson's Disease (PD).....	57
2.4.3(a)	Non-human primates (NHPs)	58
2.4.3(b)	Rodents	58
2.4.3(c)	Non-mammalian species for modelling Parkinson's Disease (PD)	59
2.4.3(c)(i)	<i>Caenorhabditis elegans</i> (<i>C. elegans</i>).....	59
2.4.3(c)(ii)	<i>Drosophila melanogaster</i>	60
2.4.3(c)(iii)	<i>Danio rerio</i>	60
2.5	Drug penetration across the Blood Brain Barrier (BBB).....	63
2.6	Adsorption, distribution metabolism, excretion, and toxicity.....	65
2.7	Computer Aided Drug Design (CADD)	67
2.7.1	Pharmacophore modelling	68
2.7.2	Validation of model development.....	69
2.8	Virtual screening	71
2.9	Molecular Docking	72
2.10	Molecular Dynamics (MD).....	73
	CHAPTER 3 MATERIALS AND METHODS.....	74
3.1	Apparatus and instruments.....	74
3.2	Chemicals and materials	74
3.3	Software and Hardwares	75
3.4	Methodology	76
3.4.1	Development of Ligand-based pharmacophore (LBP) model using α -syn protein and prolyl oligopeptidase (POP) inhibitors	76

3.4.2	Selection and validation of α -syn ligand-based model using decoy set from Zinc database.....	81
3.4.3	Re-validation of α -syn ligand-based model using decoy set from IBS, Maybridge, Hits2lead, and Arsinex databases.....	82
3.4.4	Virtual screening of the validated α -syn model.....	82
3.4.5	Selection and validation of prolyl oligopeptidase (POP) model using Gunner Henry (GH) and Enrichment factor (EF)	83
3.4.6	Virtual screening of validated prolyl oligopeptidase (POP) model using interbioscreen database	83
3.5	Molecular docking study.....	84
3.5.1	Proteins preparations.....	84
3.5.2	Preparation of retrieved Hit ligands from virtual screening process and in-house database compounds.....	87
3.5.3	Molecular docking study of the prepared ligands.....	88
3.5.4	Selection of multi-target compounds.....	89
3.6	<i>In silico</i> prediction of physicochemical, absorption, distribution, metabolism, and excretion (ADMET) study.....	90
3.7	Dynamics analysis	92
3.7.1	Molecular dynamics (MD).....	92
3.7.2	Principal component analysis (PCA).....	93
3.7.3	Residue-residue correlations	93
3.8	<i>In silico</i> oral and toxicity class prediction study of the selected ligands	94
3.9	<i>In vivo</i> study.....	95
3.9.1	<i>In vivo</i> toxicity study of the selected multi-target ligands using zebrafish (<i>Danio rerio</i>) embryo	95
3.9.2	Induction of Parkinson's Disease (PD).....	97
3.9.3	<i>In vivo</i> behavioural study of the selected multi-target compounds as inhibitors of Parkinson's disease (PD) activity using zebrafish model	98
3.9.4	Pre-treatment effects of the selected multi-target compounds to determine neuroprotective activity	98

3.9.5	Post-treatment study to determine inhibitory activity of the selected multi-targets compounds.....	100
3.10	Statistical analysis.....	101
CHAPTER 4 RESULTS.....		102
4.1	Model generation using α -syn protein inhibitors.....	102
4.1.1	Selection of α -syn Ligand-based pharmacophore model.....	103
4.1.2	Validation of α -syn ligand-based pharmacophore model (LBP).....	103
4.1.2(a)	Validation of α -syn ligand-based pharmacophore (LBP)model using test ligands and their decoy sets from Zinc database.....	103
4.1.2(b)	Validation of α -syn model using test ligands and their decoy sets from Hits2lead, Marbridge, IBS, and Asinex databases.....	105
4.1.2(c)	Virtual screening of the selected α -syn ligand-based Pharmacophore model-3.....	109
4.2	Ligand-Based Pharmacophore model generation using prolyl oligopeptidase (POP) inhibitors.....	109
4.2.1	Selection of prolyl oligopeptidase (POP) model.....	110
4.2.2	Validation of prolyl oligopeptidase (POP) model.....	110
4.2.3	Virtual screening of interbioscreen (IBS) database using prolyl oligopeptidase (POP) model-2.....	112
4.3	Molecular docking study of the 281 ligands retrieved by α -syn Model-3 on the α -syn, human tau, toxic oligomers, and prolyl oligopeptidase (POP) macromolecular targets.....	112
4.3.1	Molecular docking study of the 281 retrieved compounds on α -syn protein.....	113
4.3.2	Molecular docking scores of the 281 retrieved ligands on human tau protein.....	116
4.3.3	Molecular docking results of the 281 retrieved ligands on toxic oligomers protein.....	119
4.3.4	Molecular docking results of the retrieved 281 ligands on prolyl oligopeptidase (POP).....	123

4.3.5	Molecular docking analysis of the top fifty ligands on α -syn, human tau, toxic oligomers proteins, and prolyl oligopeptidase (POP) macromolecular targets	127
4.3.6	Molecular docking analysis of the top five compounds retrieved from prolyl oligopeptidase (POP) model-2	128
4.4	Prediction of physicochemical and pharmacokinetics analysis of the selected multi-target ligands	132
4.4.1	Adsorption, metabolism, excretion, and toxicity related to structure activity relationship (admetSAR).....	133
4.4.2	Protein kinase centric structural modeling (pkCSM) analysis of the selected multi-target screening compounds.....	135
4.4.3	Summary of absorption, distribution, metabolism, excretions, and toxicity structural activity relationship (admetSAR) and protein kinase centric structural modeling (pkCSM) pharmacokinetics analysis of the selected multi-target compounds	139
4.5	Prediction of physicochemical and pharmacokinetics analysis of the top five selected compounds from POP model-2	140
4.5.1	Physicochemical properties of the top five selected compounds from prolyl oligopeptidase (POP) model-2	140
4.5.2	Absorption, distribution, metabolism, excretions, and toxicity (ADMET) analysis of the selected top five compounds from prolyl oligopeptidase (POP) model-2 using protein kinase centric structural modeling (pkCSM) pharmacokinetics server	142
4.6	Molecular docking study of the in-house database compounds	143
4.6.1	Molecular docking score of the top fifty in-house database compounds on α -syn protein.....	144
4.6.2	Molecular docking scores of the top fifty ranked in-house ligands on human tau protein.....	147
4.6.3	Molecular docking results of the top fifty in-house ligands on toxic oligomers protein	150
4.6.4	Molecular docking results of top fifty ranked ligands from in-house database on prolyl oligopeptidase (POP).....	153
4.6.5	Molecular docking analysis of the top fifty ligands obtained from in-house database compounds on α -syn, human tau, toxic oligomers, and prolyl oligopeptidase (POP) macromolecular targets	156

4.7	Prediction of physicochemical and pharmacokinetics analysis of the selected multi-target screening ligands from top fifty docked in-house database compounds	158
4.7.1	Physicochemical properties of the selected multi-target in-house database compounds	158
4.8	<i>In silico</i> oral and class toxicity prediction study of the selected ligands	161
4.9	Dynamic analysis of the selected multi-target screening ligands	163
4.9.1	Root mean square deviation of the selected multi-target screening ligands on α -syn protein	163
4.9.2	Root mean square fluctuation of the selected multi-target screening ligands on α -syn protein	164
4.9.3	Radius of gyration analysis of the selected multi-target ligands on α -syn protein	165
4.9.4	Principal component analysis of the selected multi-target ligands on α -syn protein.....	166
4.9.5	Analysis of residue-residue correlation of the selected multi-target screening ligands on α -syn protein	167
4.10	Dynamic analysis of the selected multi-target ligands on human tau protein	168
4.10.1	Root mean square deviation of the selected multi-target screening ligands on human tau protein.....	168
4.10.2	Root mean square fluctuation of the selected multi-target ligands on human tau protein.....	169
4.10.3	Radius of gyration of the selected multi-target screening ligands on human tau protein.....	170
4.10.4	Overall internal motion as principal component analysis of the selected multi-target ligands on human tau protein	171
4.10.5	Analysis of residue-residue correlation of the selected multi-target ligands on human tau protein.....	172
4.11	Dynamics analysis of the selected multi-target screening compounds on prolyl oligopeptidase (POP).....	173
4.11.1	Root mean square deviation of the selected multi-target ligands on POP	173

4.11.2	Root mean square fluctuation of the selected multi-target ligands on prolyl oligopeptidase (POP)	174
4.11.3	Radius of gyration of the selected multi-target screening ligands on prolyl oligopeptidase (POP)	175
4.11.4	Principal component analysis of the selected multi-target ligands on prolyl oligopeptidase (POP)	176
4.11.5	Analysis of residue-residue correlation of the selected multi-target ligands on prolyl oligopeptidase (POP)	177
4.12	Dynamic analysis of the top five selected docked ligands on prolyl oligopeptidase (POP)	178
4.12.1	Root mean square deviation of the selected ligands top 5 ligands on POP	178
4.12.2	Root mean square fluctuation of the top five selected ligands on prolyl oligopeptidase (POP)	179
4.12.3	Radius of gyration analysis of the top five selected ligands-receptor complexes on prolyl oligopeptidase (POP)	180
4.12.4	Principal component analysis to determine internal dynamic motion of overall conformational trajectory of the top five selected ligands on prolyl oligopeptidase (POP)	181
4.12.5	Analysis of residue-residue correlations of the top five selected ligands on POP	182
4.13	<i>In vivo</i> toxicity and behavioural study of the selected multi-target compounds on zebrafish embryo	183
4.13.1	<i>In vivo</i> toxicity study of the selected multi-target screening ligands	184
4.13.1(a)	Mortality rate	184
4.13.1(b)	Morphological malformation at 96 hours post fertilization (hpf)	185
4.13.1(c)	Hatching rate	188
4.13.1(d)	Heart rate	189
4.14	<i>In vivo</i> toxicity study of the selected multi-target ligands from in-house database compounds	190
4.14.1	Mortality rate	190
4.14.2	Morphological malformation at 96 hours post fertilization (hpf)	191

4.14.3	Hatching rate	193
4.14.4	Heart rate per minute.....	193
4.15	Inhibition of Parkinson’s disease (PD) behaviour in zebrafish larvae <i>via in vivo</i> study	194
4.15.1	<i>In vivo</i> induction of Parkinson’s disease (PD).....	195
4.15.2	Pre- and post-treatment protocols to determine neuroprotective and inhibitory activities of selegiline as a reference compound.....	196
4.15.3	Neuroprotective activity via pre-treatment protocol for STOCK1N-51590, STOCK1N-09411, STOCK1N-68906 and STOCK1N-82941	200
4.15.3(a)	Pre-treatment protocol for STOCK1N-51590	200
4.15.3(b)	Pre-treatment protocol for STOCK1N-09411	202
4.15.3(c)	Pre-treatment protocol for STOCK1N-68906	204
4.15.3(d)	Pre-treatment protocol for STOCK1N-82941	206
4.15.4	Inhibitory activity via post-treatment experiment for STOCK1N-51590, STOCK1N-09411, STOCK1N-68906 and STOCK1N-82941	208
4.15.4(a)	Post-treatment protocol for STOCK1N-51590.....	209
4.15.4(b)	Post-treatment protocol for STOCK1N-09411.....	211
4.15.4(c)	Post-treatment protocol for STOCK1N-68906.....	213
4.15.4(d)	Post-treatment protocol for STOCK1N-82941.....	215
4.16	Neuroprotective and PD evaluation of in-house compounds	217
4.16.1	Pre-treatment protocol for B11	217
4.16.2	Pre-treatment protocol for C20	218
4.16.3	Pre-treatment protocol for D20	221
4.16.4	Inhibitory activity via post-treatment protocol for B11, C20, and D20 tetrahydro beta Carboline (TH β C) derivatives.....	223
CHAPTER 5 DISCUSSION.....		225
5.1	Development, selection, and validation of α -syn and prolyl oligopeptidase (POP) models.....	225

5.2	Virtual screening for both α -synuclein (α -syn) model-3 and prolyl oligopeptidase (POP) model-2	229
5.3	Analysis of molecular docking, binding interaction, and selection of multi-target compounds	230
5.3.1	Molecular docking, binding interactions analysis, and selection of ligands from α -synuclein (α -syn) model-3	232
5.3.2	Molecular docking, binding interactions analysis, and selection of ligands from in-house database	234
5.4	Molecular docking and binding interactions analysis of STOCK5S-72039, STOCK4S-94491, STOCK4S-02025, STOCK5S-89285, and STOCK5S-62247 ligands on prolyl oligopeptidase (POP) macromolecular target.....	237
5.5	Absorption, distribution, metabolism, excretions, and toxicity (ADMET) analysis of the multi-target ligands	240
5.5.1	Absorption, distribution, metabolism, excretions, and toxicity structure activity relationships (AdmetSAR) of the multi-target ligands	241
5.5.2	Protein kinase centric structural modeling (pkCSM) pharmacokinetic analysis of the multi-target ligands	244
5.5.3	Absorption, distribution, metabolism, excretions, and toxicity structure activity relationship (admetSAR) pharmacokinetics analysis of STOCK5S-72039, STOCK4S-94491, STOCK4S-02025, STOCK5S-89285, and STOCK5S-62247 on POP macromolecular target.....	250
5.5.4	Protein kinase centric structural modeling (pkCSM) pharmacokinetic analysis of STOCK5S-72039, STOCK4S-94491, STOCK4S-02025, STOCK5S-89285, and STOCK5S-62247 compounds on POP macromolecular target.....	251
5.6	<i>In silico</i> lethal dose fifty (LD50) toxicity analysis of the multi-target ligands using Pro Tox-II server.....	254
5.7	Dynamic analysis of the multi-target STOCK1N-51590, STOCK1N-09411, STOCK1N-82941, and STOCK1N-68906 compounds.....	256
5.8	Dynamic analysis of STOCK5S-72039, STOCK4S-94491, STOCK4S-02025, STOCK5S-89285, and STOCK5S-62247 ligands on POP macromolecular target	259
5.9	<i>In vivo</i> toxicity of the multi-target ligands using zebrafish model	263
5.9.1	Mortality rate	263

5.9.2	Morphological changes	264
5.9.3	Hatching rate analysis	265
5.9.4	Heart rate analysis	267
5.10	<i>In vivo</i> Parkinson's disease (PD) induction and behavioural analysis on zebrafish larvae	268
5.10.1	Validation analysis of rotenone-induced PD on zebrafish larvae.....	269
5.10.2	Neuroprotective and inhibitory activities of selegiline as reference compound.....	270
5.10.3	<i>In vivo</i> neuroprotective activity analysis of STOCK1N-51590, STOCK1N-09411, STOCK1N-82941, and STOCK1N- 68906.....	271
5.10.4	<i>In vivo</i> inhibitory activity analysis of the selected multi-target compounds.	274
5.11	Novelty of the study	276
CHAPTER 6 CONCLUSION AND FUTURE RECOMENDATIONS.....		278
6.1	Conclusion	278
6.2	Recommendation for Further Research	281
REFERENCES.....		283
APPENDICES		
LIST OF PUBLICATIONS		

LIST OF TABLES

	Page
Table 2.1	Classes and symptoms of drugs used in management of PD. Adapted and Reproduced from Amstrong et al., (2020), Licenced under CC BY 4.0.)..... 39
Table 3.1	List of Instruments or apparatus used in the experiment 74
Table 3.2	List of chemicals or materials used in the experiment..... 74
Table 3.3	List of software used and their importance..... 76
Table 3.4	Chemical structures of compounds used as training set to generate α -syn pharmacophore models with various IC ₅₀ 76
Table 3.5	Chemical structures of compounds used as training set to generate the POP pharmacophore models having various IC ₅₀ 78
Table 3.6	admetSAR parameters used to screen the multi-target screening compounds..... 90
Table 3.7	Criteria for screening the selected multi-target binding ligands using pkCSM pharmacokinetics server..... 91
Table 4.1	List of the models and their pharmacophore fit scores generated on α -syn protein..... 102
Table 4.2	Validation parameters of α -syn model using external ligands having shared feature pharmacophore model 104
Table 4.3	Validation parameters of the shared pharmacophore feature of α -syn model vs decoys from different databases 106
Table 4.4	List of POP models and their pharmacophore fit scores generated from POP inhibitors..... 109
Table 4.5	Validation parameters of the shared feature of selected POP pharmacophore model..... 111
Table 4.6	Molecular docking results of the top fifty docked 281 retrieved ligands and reference compounds on α -syn protein..... 113
Table 4.7	Molecular docking results of the top fifty docked 281 ligands and reference compounds on human tau protein 116
Table 4.8	Molecular docking results of the top fifty docked 281 ligands and reference compounds on toxic oligomers..... 119

Table 4.9	Binding activity of the top fifty docked 281 ligands and reference compounds on POP	123
Table 4.10	List of the selected ligands having multi-target binding activity.....	127
Table 4.11	Binding activity results on POP for the top fifty, docked 177 ligands from POP model-2 and reference compounds	128
Table 4.12	Chemical properties of the multi-target screening ligands	133
Table 4.13	admetSAR properties of the selected multi-target screening ligands	134
Table 4.14	pk-CSM analysis results for the selected of the multi-target screening ligands.....	136
Table 4.15	Final selected multi-target screening ligands that pass both admetSAR and pkCSM pharmacokinetics analysis.....	139
Table 4.16	Chemical properties of the top five selected compounds from POP model-2	141
Table 4.17	admetSAR properties of the top five selected compounds from POP model-2	141
Table 4.18	ADMET properties of the top five selected compounds from POP model-2 and reference compound using pkCSM server.....	142
Table 4.19	Molecular docking scores and energy for top fifty in-house ligands on α -syn protein.....	144
Table 4.20	Molecular docking and energy scores of the top fifty in-house ligands on human tau protein.....	147
Table 4.21	Molecular docking and energy scores of the top fifty in-house ligands on toxic oligomers protein.....	150
Table 4.22	Molecular docking and energy scores of the top fifty in-house ligands on POP	153
Table 4.23	Ligands from in-house database having multi-target binding activity on four targets.	156
Table 4.24	Chemical properties of the selected compounds from in-house database compounds	158
Table 4.25	admetSAR properties of the selected in-house database compounds	159
Table 4.26	ADMET properties of the selected in-house database compounds and reference compound using pkCSM server.....	159

Table 4.27	Prediction of oral rat lethal dose fifty (LD50) values and the toxicity class of the selected multi-target compounds	161
Table 4.28	Oral rat LD50 values and the toxicity class of the top five selected compounds from POP model-2.....	162
Table 4.29	Oral rat LD50 values and the toxicity class of the selected multi-target ligands from in-house database compounds	162
Table 4.30	The percentage mortality rate of the selected multi-target ligands on zebrafish embryo at different hpf.....	185
Table 4.31	Morphological malformation of the multi-target screening ligands on zebrafish embryos at 96 hpf	186
Table 4.32	The percentage mortality rate of the selected multi-target ligands obtained from in-house database compounds on zebrafish embryo at different hpf.....	190
Table 4.33	Morphological malformation on zebrafish embryos at 96 hpf	191

LIST OF FIGURES

	Page
Figure 1.1	The process of amyloid fibril formation through oligomerization. Reproduced and adapted from Baldwin <i>et al.</i> , 2011, Licenced under CC BY 4.0..... 3
Figure 1.2	Compounds use to manage PD symptoms..... 5
Figure 1.3	Summary of the research flow chart..... 9
Figure 2.1	Structure of human micelle-bound α -syn retrieved from protein data Bank demonstrating its various domain..... 15
Figure 2.2	Structure of α -syn showing the NAC domain..... 16
Figure 2.3	Functions of α -syn and its role in disease state. Reproduced and adapted from Snead and Eliezer 2014, Licenced under CC BY 4.0..... 18
Figure 2.4	Chemical structure of phenothiazine and its derivatives 23
Figure 2.5	Chemical structures of polyphenols compounds as inhibitors of α -syn protein..... 25
Figure 2.6	Illustration of how crocin prevents amyloid fibril formation of E46K 26
Figure 2.7	Some naturally occurring POP inhibitors 32
Figure 2.8	Chemical structure of 4-phenylbutanoyl-1-prolyl-2(S)-cyanopyrrolidine (KYP-2047) a potent inhibitor of α -syn protein 33
Figure 2.9	The process of α -syn aggregation under physiological conditions promoting SNARE-complex assembly and tetramers that can resist abnormal aggregation. (Adopted and reproduced from Du <i>et al.</i> , (2020), Licenced under CC BY 4.0.) 35
Figure 2.10	Chemical structures of some dopamine agonist..... 40
Figure 2.11	Chemical structures of some MOBI..... 42
Figure 2.12	Some COMT inhibitors..... 44
Figure 2.13	Structure of some SSRIs members 47
Figure 2.14	Structure of some AChI members..... 48

Figure 2.15	Structure of amantadine	50
Figure 2.16	Skeleton of carbolines: (A) indicated the β C while (B) shows the TH β C skeleton having various positions	51
Figure 2.17	Structure of amantadine	54
Figure 2.18	Structure of 6-OHDA and dopamine	55
Figure 2.19	Structure of rotenone.....	56
Figure 2.20	Structure of N,N'-dimethyl-4,4'-bipyridium dichloride (paraquat)	57
Figure 2.21	Illustrating the transparent nature of Zebrafish. (A) shows the larval and (B) adult Zebrafish organs. (Adapted and reproduced from Bhagat et al., (2020), Licenced under CC BY 4.0.).....	62
Figure 3.1	Induction of PD in zebrafish larvae using rotenone.....	98
Figure 3.2	Demonstration of pre- and post-treatment protocols using the selected multi-target compounds on PD behavioural activity.	99
Figure 3.3	Pre-treatment protocol and induction of PD on zebrafish larvae.....	100
Figure 3.4	Post-treatment protocol and induction of PD on zebrafish larvae.....	101
Figure 4.1	The α -syn model generated. (A) the model generated with superimposed hits ligands, (B) The skeleton of the LBP model showing various features generated, consisting of four HBA (red), five HBD (green), and one AR (blue).....	103
Figure 4.2	The ROC of α -syn generated model validated using test ligands vs decoys sets from zinc database	105
Figure 4.3	The ROC of α -syn model validated using decoys from Hits2lead database	107
Figure 4.4	The ROC of α -syn model validated using decoys from IBS database.....	107
Figure 4.5	The ROC of α -syn model validated using decoys from Maybridge database	108
Figure 4.6	The ROC of α -syn model validated using decoys from Arsinex database.....	108
Figure 4.7	The POP model generated. (A) the model generated with superimposed hits ligands, (B) The skeleton of the ligand-	

	based pharmacophore model showing various features generated, consisting of one H (yellow), one PI (finger-like blue), two Ar (ring blue), and two HBA (red)	110
Figure 4.8	The ROC of the generated POP model validated using external validators	112
Figure 4.9	Showcases the binding interactions of the selected compounds from α -syn model-3 with the α -syn protein: (A) 3D illustrations of the ligands at the binding pocket site, (B) 2D interactions of the selected ligands with various AA residues.....	116
Figure 4.10	Binding interactions of the selected compounds from α -syn model-3 on human tau protein (A) 3D illustrations of the ligands at the binding pocket site, (B) 2D interactions of the selected ligands with various AA residues	119
Figure 4.11	Binding interactions of the selected ligands from α -syn model-3 on toxic oligomers protein (A) 3D illustrations of the ligands at the binding pocket site, (B) 2D interactions of the selected ligands with various AA residues	123
Figure 4.12	Binding interactions of the selected compound from α -syn model-3 on POP (A) 3D illustrations of the ligands at the binding pocket site, (B) 2D interactions of the selected ligands with various AA residues	126
Figure 4.13	Binding interactions of the selected top five compounds from POP model-2 on POP protein (A) 3D illustrations of the ligands at the binding pocket site, (B) 2D interactions of the selected ligands with various AA residues	132
Figure 4.14	Binding interactions of the selected in-house database and reference compounds on α -syn protein (A) 3D illustrations of the ligands at the binding pocket site, where the dots blue line captured ligand and the ash background indicated the receptor binding site (B) 2D interactions of the selected ligands with various AA residues	147
Figure 4.15	Binding interactions of the reference compounds on human tau protein (A) 3D illustrations of the ligands at the binding pocket site, where the ash background indicated the receptor binding site (B) 2D interactions of the selected ligands with various AA residues	150
Figure 4.16	Binding interactions of the selected ligands and reference compounds on toxic oligomers protein (A) 3D illustrations of the ligands at the binding pocket site, where the blue dots lines indicate ligand binding site and ash background indicated the receptor binding site (B) 2D interactions of the selected ligands with various AA residues	153

Figure 4.17	Binding interactions of the reference compounds on POP (A) 3D illustrations of the ligands at the binding pocket site, where the ash background indicated the receptor binding site (B) 2D interactions of the selected ligands with various AA residues.....	156
Figure 4.18	RMSD plots of the selected multi-target screening ligand-receptor complexes on α -syn protein. The X-axis represents time in ns, while the Y-axis represents the RMSD value in Angstrom.....	164
Figure 4.19	RMSF of the selected multi-target ligand-receptor complexes on α -syn protein. The X-axis represents AA residues, while the Y-axis represents the RMSD value in Angstrom.....	165
Figure 4.20	The Rg analysis of the selected multi-target ligand-receptor complexes on α -syn protein. The X and Y axis represents the number of frames and radius of gyration respectively.....	166
Figure 4.21	The PCA analysis of the selected multi-target ligand-receptor complexes on α -syn protein, where the blue and red color indicated highly correlated and less correlated interactions at the receptor binding site.....	167
Figure 4.22	The DCCM analysis revealing positive and negative correlation motion among the residues for the selected multi-target ligands and reference compounds on α -syn protein.....	168
Figure 4.23	RMSD plots of the selected ligand-receptor complexes on human tau protein. The X-axis represents time in ns, while the Y-axis represents the RMSD value in Angstrom.....	169
Figure 4.24	RMSF of the selected multi-target ligands and reference compounds on human tau protein.	170
Figure 4.25	The Rg analysis of the selected multi-target ligands and reference compounds on human tau protein. The X and Y axis represents the number of frames and radius of gyration respectively.	171
Figure 4.26	The PCA analysis of the selected multi-target ligand-receptor complexes on human tau protein, where the blue and red color indicated highly correlated and less correlated interactions at the receptor binding site.....	172
Figure 4.27	The dynamic cross-correlated matrix analysis revealing the collective positive and negative correlation motion among the residues for the selected multi-target ligands receptor complexes on human tau protein.	173
Figure 4.28	RMSD plots of the selected multi-target ligand-receptor on POP. The X-axis represents time in ns, while the Y-axis represents the RMSD value in Angstrom	174

Figure 4.29	RMSF of the selected multi-target screening ligands and reference compounds on POP.	175
Figure 4.30	The Rg analysis of the selected multi-target ligands and reference compounds on POP. The X and Y axis represents the number of frames and radius of gyration respectively.....	176
Figure 4.31	The PCA analysis of the selected multi-target ligand-receptor complexes on POP, where the blue and red color indicated highly correlated and less correlated interactions at the receptor binding site.....	177
Figure 4.32	The dynamic cross-correlated matrix analysis revealing the collective positive and negative correlation motion among the residues for the selected multi-target ligands and reference compounds on POP.....	178
Figure 4.33	RMSD plots of the top five ligand-receptor complexes from POP and reference GSK552 on POP. The X-axis represents time in ns, while the Y-axis represent the RMSD value in Angstrom.....	179
Figure 4.34	RMSF of the top five selected ligand-receptor complexes from POP and reference GSK552. The X-axis represents residues, while the Y-axis represent the RMSD value in Angstrom.	180
Figure 4.35	The Rg analysis of the top five ligand-receptor complexes from POP and reference GSK552. The X-axis represents number of frames, while the Y-axis represent the radius of gyration in Angstrom.....	181
Figure 4.36	PCA Analysis of the top five selected ligand-receptor complexes from POP.	182
Figure 4.37	dynamic cross-correlated matrix analysis of the top five selected ligands from POP revealing the collective positive and negative correlation motion among the residues of the ligand-receptor complexes.	183
Figure 4.38	Morphological observation of the selected multi-target screening compounds on zebrafish embryo at 96 hpf.....	188
Figure 4.39	Hatching rate of zebrafish embryos exposed to multi-target selected ligands at 72 and 96 hpf.	188
Figure 4.40	Heartbeat per minute of zebrafish embryos exposed to multi-target selected ligands at 96 hpf. Data expressed as the mean \pm SD $p < 0.05$, $n = 3$	189
Figure 4.41	Morphological observations of the selected multi-target compounds obtained from in-house database compounds on zebrafish embryo at 96 hpf.....	192

Figure 4.42	Hatching rate of zebrafish embryos exposed to multi-target selected ligands from in-house database compounds at 72 and 96 hpf.	193
Figure 4.43	Heartbeat per minute of the zebrafish embryo exposed to the selected multi-target compounds from in-house database. Data expressed as the mean \pm SD $p < 0.05$, $n = 3$	194
Figure 4.44	Plots of zebrafish larvae's behaviour when exposed to rotenone for inducing PD. (A) indicates the locomotor activity while (B) indicates the total distance covered by the Zebrafish larvae when compared with negative and solvent controls. Data expressed as the mean \pm SD $p < 0.05$, $n = 3$	195
Figure 4.45	Neuroprotective activity of selegiline via pre-treatment protocol in zebrafish larvae. (A) indicates the locomotor activity while (B) indicates the total distance covered by the zebrafish larvae when pre-treated with Reference compounds. Data expressed as the mean \pm SD $p < 0.05$, $n = 3$	197
Figure 4.46	Neuroprotective trajectories for PD induction with rotenone when pre-treated with reference compounds	198
Figure 4.47	Inhibitory activity of selegiline via post-treatment protocol in zebrafish larvae. (A) indicates the locomotor activity while (B) indicates the total distance covered by the zebrafish larvae when post-treated with selegiline. Data expressed as the mean \pm SD $p < 0.05$, $n = 3$	199
Figure 4.48	Neuroprotective activity trajectories of zebrafish larvae for reference controls when challenged with rotenone via post-treatment protocol.	200
Figure 4.49	Neuroprotective activity plot via pre-treatment protocol for STOCK1N-51590 on zebrafish larvae (A) indicates the locomotor activity of the zebrafish larvae. (B) showed the total distance travelled by the zebrafish larvae. Data expressed as the mean \pm SD $p < 0.05$, # not determined, $n = 3$	201
Figure 4.50	The typical track trajectories indicating total distance travelled when larvae were pre-treated with STOCK1N-51590 at various concentrations	202
Figure 4.51	The plot of neuroprotective activity via pre-treatment protocol for STOCK1N-09411 on zebrafish larvae (A) indicates the locomotor activity of the zebrafish larvae. (B) showed the total distance travelled by the zebrafish larvae. Data expressed as the mean \pm SD $p < 0.05$, $n = 3$	203
Figure 4.52	The typical track trajectories indicating total distance travelled when larvae were pre-treated with STOCK1N-09411 at various concentrations	204

Figure 4.53	The plot of neuroprotective activity via pre-treatment protocol for STOCK1N-68906 on zebrafish larvae (A) indicates the locomotor activity of the zebrafish larvae. (B) showed the total distance travelled by the zebrafish larvae. Data expressed as the mean \pm SD $p < 0.05$, $n = 3$	205
Figure 4.54	The typical track trajectories indicating total distance travelled when larvae were pre-treated with STOCK1N-68906 at various concentrations.	206
Figure 4.55	The plot of neuroprotective activity via pre-treatment protocol for STOCK1N-82941 on zebrafish larvae (A) indicates the locomotor activity of the zebrafish larvae. (B) showed the total distance travelled by the zebrafish larvae. Data expressed as the mean \pm SD $p < 0.05$, # not determined, $n = 3$	207
Figure 4.56	The typical trajectories track indicating the total distance travelled when larvae were pre-treated with STOCK1N-82941 at various concentrations.....	208
Figure 4.57	The inhibitory activity via post-treatment protocol plot STOCK1N-51590 on zebrafish larvae (A) indicates the locomotor activity of the zebrafish larvae. (B) showed the total distance travelled by the zebrafish larvae. Data expressed as the mean \pm SD $p < 0.05$, $n = 3$	210
Figure 4.58	The typical trajectories track showing the total distance travelled when larvae were exposed to rotenone and post-treated with STOCK1N-51590 at various concentrations	211
Figure 4.59	The inhibitory activity via post-treatment protocol plot for STOCK1N-09411 on zebrafish larvae (A) indicates the locomotor activity of the zebrafish larvae. (B) showed the total distance travelled by the zebrafish larvae. Data expressed as the mean \pm SD $p < 0.05$, # not determined, $n = 3$	212
Figure 4.60	The typical trajectories track showing the total distance travelled when larvae were exposed to rotenone and post-treated with STOCK1N-09411 at various concentrations	213
Figure 4.61	The inhibitory activity results via post-treatment protocol for STOCK1N-68906 on zebrafish larvae (A) indicates the locomotor activity of the zebrafish larvae. (B) showed the total distance travelled by the zebrafish larvae. Data expressed as the mean \pm SD $p < 0.05$, $n = 3$	214
Figure 4.62	The typical trajectories track showing the total distance travelled when larvae were exposed to rotenone and post-treated with STOCK1N-68906 at various concentrations	215
Figure 4.63	The results of inhibitory activity via post-treatment protocol for STOCK1N-82941 on zebrafish larvae (A) indicates the	

	locomotor activity while (B) showed the total distance travelled by the zebrafish larvae. Data expressed as the mean \pm SD $p < 0.05$, $n = 3$	216
Figure 4.64	The typical trajectories track showing the total distance travelled when larvae were exposed to rotenone and post-treated with compound-D at various concentrations.....	217
Figure 4.65	The results of neuroprotective activity via pre-treatment protocol plots for B11 ligand on zebrafish larvae (A) indicates the locomotor activity while (B) showed the total distance travelled by the zebrafish larvae. Data expressed as the mean \pm SD $p < 0.05$, # not determined, $n = 3$	218
Figure 4.66	The results of neuroprotective activity via pre-treatment protocol plots for C20 ligand on zebrafish larvae (A) indicate the locomotor activity while (B) showed the total distance travelled by the zebrafish larvae. Data expressed as the mean \pm SD $p < 0.05$, # not determined, $n = 3$	220
Figure 4.67	The typical trajectories track showing the total distance travelled when larvae were pre-treated with ligand C20 at various concentrations and exposed to rotenone.....	221
Figure 4.68	The results of neuroprotective activity via pre-treatment protocol plots for ligand D20 on zebrafish larvae (A) indicates the locomotor activity while (B) showed the total distance travelled by the zebrafish larvae. Data expressed as the mean \pm SD $p < 0.05$, $n = 3$	222
Figure 4.69	The typical trajectories track showing the total distance travelled when larvae were pre-treated with ligand D20 at various concentrations and exposed to rotenone.....	223
Figure 4.70	The results of inhibitory activity via post-treatment protocol plots for ligands B11, C20, and D20 on zebrafish larvae (A) indicates the locomotor activity while (B) showed the total distance travelled by the zebrafish larvae. Data expressed as the mean \pm SD $p < 0.05$, # not determined, $n = 3$	224

LIST OF SYMBOLS

α	Alpha
β	Beta
p	Probability
$\mu\text{g/L}$	Microgram Per Liter
μL	Micro Liter
μM	Micro Molar
π	Pie
%	Percentage
>	Greater than
<	Less than
/	Per
kg	Kilogram
LogBB	Blood Brain Barrier Permeability
LogP	Lipophilicity
mm/	Milli Meter
mol	Molarity
QLogS	Solubility
sec	Second

LIST OF ABBREVIATIONS

AA	Amino Acid residues
AAAD	Aromatic Amino Acid Decarboxylase
A β	Amyloid beta
AChI	Acetylcholinestrane Inhibitors
AD	Alzheimer's disease
ADMET	Adsorption, distribution, metabolism, excretion, and toxicity
ALP	Autophagy-Lysosomal Pathways
ALS	Amyotrophic lateral sclerosis
AMBER	Assisted Model Building with Energy Refinement
AOT	Acute Oral Toxicity
AR	Aromatic Ring
ATP	Adenosine Triphosphate
AUC	Area Under The Curve
α -syn	α -synuclein
BBB	Blood-Brain Barrier
CADD	Computer Aided Drug Design
CMT	Carrier-Mediated Transport
CNS	Central Nervous System
COMT	Catechol-O-methyl Transferase Enzyme
COMTI	Catechol-O-Methyltransferase Inhibitors
CVD	Cardiovascular Diseases
CYP	Cytochrome P450 Enzyme
3D	Three-Dimensional
DA	Dopamine Agonist

DAWS	Dopamine Withdrawal Symptoms
DBS	Deep Brain Simulation
DCCM	Dynamic Cross Correlated Matrix
DIP	Drug-Induced Parkinsonism
DMSO	Dimethyl Sulfoxide
DNA	Deoxyribonucleic Acid
DLB	Dementia with Lewy's body
DPP-IV	Dipeptidyl Peptidase IV
EF	Enrichment Factor
ER	Endoplasmic reticulum
ELISA	Enzyme-Linked Immunosorbent Assay
FAD	Food and Drug Administration
FN	False-negative
FAP	Fibroblast Activation Protein alpha
FP	False-positive
GH	Goodness of hit score or Gunner Henry's score
GIP	Gastric Inhibitory Polypeptide
GLP-1	Glucagon-like Petide-1
GSK552	Glycogen Synthase Kinase-552
H	Hydrogen
HBA	Hydrogen Bond Acceptors
HBD	Hydrogen Bond Donors
6-OHDA	6-Hydroxydopamine
HD	Huntington's disease
hERG	Human Ether A-Go-Ago-Related Gene
HIA	Human Intestinal absorption
HOB	Human Oral Bioavailability

hpf	Hours Post-Fertilization
hrs	Hours
Ht	Total Hits
IA	Intestinal Absorption
IC ₅₀	Minimum Inhibitor Concentration
IBS	interbioscreen
IDP	Intrinsically Disordered Proteins
IDPD	Idiopathic Parkinson's Disease
IPS	Institute of Postgraduate School
LAT1	large type amino acid transporter 1
LBDD	Ligand-Based Drug Design
LBP	Ligand-Based Pharmacophore
LBs	Lewy Bodies
LD50	Lethal Dose 50 %
LN _s	Lewy Neutrals
LRRK2	Leucine-Rich Repeat Kinase 2
LogP	Logarithm of lipophilicity
LogS	Logarithm of Solubility
LOEL	Lowest Observed Adverse Effect Level
MD	Molecular Dynamics Simulation
MMGBSA	Molecular Mechanics Generalized Born Surface Area
MOA	Monoamine Oxidase Enzyme
MOBI	Monoamine Oxidase Inhibitors
MPTP	1-methyl-4-phenyl-1,3,4,6-tetrahydropyridine
MW	Molecular Weight
ND _s	Neurodegenerative diseases
NFT _s	Neurofibrillary Tangles

NHP	None-Human Primates
NRB	Number of Rotatable Bonds
OECD	Organization For Economic Cooperation and Development
PCA	Principal Component Analysis
PC	Principal Component
PDB	Protein Data Bank
P-gp	Permeability Glycoprotein
pkCSM	Protein Kinase Centric Structural Modeling
POD	Phosphorylative Oxidative Deficiencies
POP	Prolyl Oligopeptidase
PP2A	Protein Phosphatase 2A
PTM	Post-translational Modification
Rg	Radius of Gyration
RDf	Radial Distribution Function
RMSD	Root Mean Square Deviation
RMSF	Root Mean Square Fluctuation
RNA	Ribonucleic Acid
ROC	Receiver Operating Characteristics
S9	Serine Protease Enzyme
SBDD	Structure-Based Drug Design
SE	Sensitivity
Sel	Selegiline
SP	Specificity
SPECT	Single-Photon Emission Computed Tomography
SPPS	Statistical Package For Social Sciences
SSRI	Serotonin Re-uptake Inhibitors
TCA	Tricyclic Antidepressants

TF	True Positive
TH β C	Tetrahydro- β -Carboline
TN	True negatives
TP	True Positive
TPSA	Topological Polar Surface Area
UPP	Ubiquitin-Proteasome Pathway
USM	Universiti Sains Malaysia
VP	Vascular Parkinsonism
WT	Wild Type
XP	Extra Precision

LIST OF APPENDICES

- Appendix A1 List of the nine α -syn. models that failed validation status using EF and GH scores
- Appendix A1 List of active ligands used for validation of selected α -syn. model
- Appendix A2 List of 25 active ligands used for validation of α -syn. model vs decoy from four databases
- Appendix A3 List of active ligands used for validation of POP model vs decoy sets
- Appendix A4 List of the nine POP models that failed validation status using EF and GH scores
- Appendix B1 Breeding of Zebrafish
- Appendix B2 Protocol for toxicity study of Zebrafish embryo
- Appendix B3 Protocol for inducing PD and treatment in Zebrafish Larvae
- Appendix C1 Statistical results for the selected multi-target compounds, STOCK1N-51590, STOCK1N-09411, STOCK1N-82941, and STOCK1N-68906
- Appendix C2 Statistical results for the selected multi-target ligands from in-house database compounds (C20 and D20)
- Appendix D Prediction of organ toxicity and cytotoxicity endpoints of the selected multi-target compounds
- Appendix E1 Morphological observations for multi-target selected STOCK1N-51590 ligand at different concentrations and hpf.
- Appendix E2 Morphological observations for multi-target selected STOCK1N-09411 ligand at different concentrations and hpf.
- Appendix E3 Morphological observations for multi-target selected STOCK1N-68906 ligand at different concentrations and hpf.
- Appendix E4 Morphological observations for multi-target selected STOCK1N-82941 ligand at different concentrations and hpf.
- Appendix F1 Morphological observations for multi-target selected ligand, B11 at different concentrations and hpf
- Appendix F2 Morphological observations for multi-target selected compound, C20 at different concentrations and hpf

Appendix F3 Morphological observations for multi-target selected compound,
D20 at different concentrations and hpf

**PENEMUAN PERENCAT PELBAGAI SASARAN DALAM PENYAKIT
PARKINSON MENGGUNAKAN PEMODELAN MOLEKUL,
PEMPROFILAN ADMET SECARA *IN SILICO* DAN ANALISIS TINGKAH
LAKU LARVA IKAN ZEBRA**

ABSTRAK

Penyakit Parkinson (PD) adalah gangguan neurodegeneratif yang lazimnya akan membawa kepada kehilangan upaya. Penyelidikan ini bertujuan untuk mengenal pasti perencat yang menyasarkan pelbagai protein yang terlibat dalam perkembangan PD. Model farmakofor berasaskan ligan (LBP) telah dibangun dan disahkan dengan menggunakan perencat protein α -synuclein (α -syn) dan perencat enzim prolil oligopeptidase (POP). LBP Model-3 untuk α -syn dan model-2 untuk perencat POP telah dipilih berdasarkan teknik skor Gunner Henry dan faktor Pengayaan. Model ini digunakan bagi menyaring perencat PD yang berpotensi. Model-3 α -syn mempunyai sifat farmakoforik yang terdiri daripada 4 penerima ikatan hidrogen, 5 penderma ikatan hidrogen, dan 1 cincin aromatik dan digunakan bagi menyaring pangkalan data Maybridge, IBS, dan Arsinex yang keseluruhannya mempunyai 254,870 sebatian. Model-2 POP pula mempunyai ciri 1 kumpulan hidrofobik, 1 kumpulan terion positif, dan 2 cincin aromatic dan digunakan bagi menyaring pangkalan data IBS, yang terdiri daripada 69,543 sebatian. Model-3 dan Model-2, masing-masing berjaya mengenal pasti 281 dan 177 sebatian melalui saringan maya. Pengedokan molekul 281 perencat α -syn terhadap empat protein sasaran berkaitan PD iaitu, α -syn (PDB:1XQ8), tau manusia (PDB:4EOM), oligomer toksik (PDB:5F1T), dan POP (PDB:3DDU) berjaya mengenal pasti 11 sebatian multi-sasaran dan 4 sebatian iaitu, STOCK1N-51590, STOCK1N-09411, STOCK1N-89241, STOCK1N-68906 dipilih bagi penilaian

biologi selepas analisis ADMET dijalankan. Bagi 177 sebatian yang disaring daripada POP Model-2, 5 sebatian teratas yang dipilih menunjukkan secara *in siliko* mereka berpotensi menghasilkan kesan toksisiti dan juga kebolehtelapan melepasi BBB yang terhad, juga tidak dipilih bagi penilaian biologi. Pendedokan molekul terhadap 270 sebatian berasaskan THBC berjaya mengenal pasti 14 sebatian multi-sasaran, dan 3 sebatian iaitu, B11, C20, D20 telah dipilih. Kesemua tujuh sebatian yang dipilih adalah tidak toksik terhadap embrio ikan zebra. STOCK1N-51590, STOCK1N-09411, STOCK1N-82941, dan STOCK1N-68906 menunjukkan kedua-dua aktiviti neuroprotektif dan pembalikan terhadap tingkah laku berkaitan PD. Bagi terbitan THBC pula, C20 dan D20 menunjukkan aktiviti neuroprotektif tetapi tidak menunjukkan pembalikan tingkah laku berkaitan PD. Manakala B11 tidak menunjukkan sebarang aktiviti neuroprotektif atau pembalikan tingkah laku. Kajian ini mengenal pasti beberapa perencat berpotensi yang menyasarkan pelbagai protein yang terlibat dalam perkembangan PD dan memerlukan penilaian lanjut.

**DISCOVERY OF MULTI-TARGETING INHIBITORS IN PARKINSON'S
DISEASE USING MOLECULAR MODELLING, *IN SILICO* ADMET
PROFILING, AND BEHAVIOURAL ANALYSIS OF ZEBRAFISH LARVAE**

ABSTRACT

Parkinson's disease (PD) is a neurodegenerative disorder that usually leads to physical disability. This research aims to identify inhibitors targeting multi-target proteins involved in the progression of PD. Ligand-based pharmacophore models (LBP) were developed and validated using α -synuclein (α -syn) protein and prolyl oligopeptidase (POP) enzyme inhibitors. LBP model-3 for α -syn and model-2 for POP inhibitors were selected based on the Gunner Henry score and Enrichment factor techniques. These models were employed for the screening of potential PD inhibitors. The α -syn model-3 has pharmacophoric properties consisting of 4 hydrogen bond acceptors, 5 hydrogen bond donors and 1 aromatic ring and is used to screen the Maybridge, IBS, and Arsinex databases, which in total have 254,870 compounds. The POP model-2, on the other hand, features 1 hydrophobic group, 1 positive ionized group, and 2 aromatic rings and is used to screen the IBS database, which consists of 69,543 compounds. Model-3 and Model-2, respectively, managed to identify 281 and 177 compounds through the virtual screenings. Molecular docking of 281 α -syn inhibitors against the four PD-related protein targets of α -syn (PDB:1XQ8), human tau (PDB:4EOM), toxic oligomer (PDB:5F1T), and POP (PDB:3DDU) managed to identify 11 multi-target compounds and only 4 compounds namely, STOCK1N-51590, STOCK1N-09411, STOCK1N-89241, STOCK1N-68906 were selected for biological assessment after the ADMET evaluation. Of the 177 compounds from POP model-2, the top five compounds selected showed *in silico* toxicity potential and limited blood

brain barrier permeability and therefore were not selected for biological assessment. Molecular docking of 270 tetrahydro beta carboline (TH β C) in-house data-based compounds successfully identified 14 multi-target compounds, and 3 compounds, B11, C20, and D20 were chosen. All seven compounds selected are non-toxic to zebrafish embryos compared to the reference compound, doxorubicin. STOCK1N-51590, STOCK1N-09411, STOCK1N-82941, and STOCK1N-68906 showed both neuroprotective activity and reversal of PD-related behaviours. For TH β C derivatives, C20 and D20 showed neuroprotective activity but without reversal of PD-related behaviour. On the other hand, B11 did not show any neuroprotective or reversal activities. The study successfully identified several potential inhibitors targeting multiple proteins involved in the progression of PD and warranted further evaluation.

CHAPTER 1

INTRODUCTION

1.1 Background

Globally, there is a growing prevalence of neurodegenerative diseases (NDs) that contribute to years of life lived with physical disability, particularly among the elderly population. Projections suggest that by 2060, the global count of individuals affected by NDs could surpass 150 million (Armstrong, 2020).

NDs constitute a cluster of disorders affecting the central nervous system, causing a gradual breakdown of dopaminergic neurons. These conditions are marked by a progressive decline in the structure and function of neurons, evident through the emergence of distinctive features that are often recognized as classical indications of the disorders (Bougea, 2021). The impact on dopaminergic neurons results in a variety of signs and symptoms, which vary based on the specific structural protein involved.

Various types of NDs exist, encompassing conditions such as Parkinson's disease (PD), Alzheimer's disease (AD), spinal cord injury (SCI), and amyotrophic lateral sclerosis (ALS), among others. These NDs present serious concern for brain-related illnesses, particularly among the elderly population. Broadly, NDs are categorized into familial and sporadic forms. Familial cases entail a familial history of the disorders, enabling the creation of *in vitro* and *in vivo* disease models. An early trigger for familial PD has been identified as the duplication or triplication of three crucial genes (A30P, A53T, and E46K) within the α -synuclein (α -syn) protein. Sporadic NDs involve multiple genetic factors that intersect at the molecular level pathways (Rawji et al., 2020). While the exact origins and mechanisms of PD remain unclear, a multitude of diverse pathophysiologies contribute to its various clinical

presentations. Notably, α -syn and amyloid beta ($A\beta$) are characteristic of PD and AD, respectively (Armstrong, 2019; Bordoni et al., 2020). The precise causation of PD remains elusive, but postulated mechanisms encompass (i) a blend of risk factors, (ii) advancing age, (iii) impacts on neuroanatomical pathways, (iv) degeneration of dopaminergic neurons culminating in the formation of pathogenic proteins, (v) gradual diffusion of these pathogenic proteins to neighboring neurons, and subsequently, (vi) the convergence of heterogeneous pathologies leading to the depletion of 3-hydroxytyramine (dopamine) (Armstrong, 2020; Voet et al., 2019).

The misfolding and aggregation of proteins, resulting in the formation of pathogenic structures, represent a prevalent process underlying the progression of PD and various other NDs. Each of these disorders is associated with a specific misfolded and aggregated protein, such as α -syn in PD, amyloid beta ($A\beta$) and tau protein (TP) in AD, huntingtin in Huntington's disease (HD), and prion protein in prion disease. Initially, the accumulation of these proteins, starting from individual monomers, leads to the creation of a highly organized conformational structure known as a β -sheet. Subsequent rearrangements of the β -sheet structure into diverse forms initiate the process of oligomerization, resulting in the formation of oligomers. These oligomers, varying in size and shape, then progress to aggregate into protofibrils. Through subsequent elongation processes, these protofibrils evolve into more complex structures known as amyloid fibrils (Armstrong, 2020; Voet et al., 2019).

Amyloid fibrils often serve as the pathological and structural hallmark in the majority of NDs. Throughout this process, a balance is upheld between oligomers, protofibrils, and amyloid fibrils. Fig. 1.1 illustrates the progression from monomers to the formation of amyloid fibril structures. The amyloid fibrils display distinct

tendencies to manifest diverse structural, physiological, and functional attributes across various NDs disorders (Ikeda and Yamada, 2010; Tittelmeier et al., 2020).

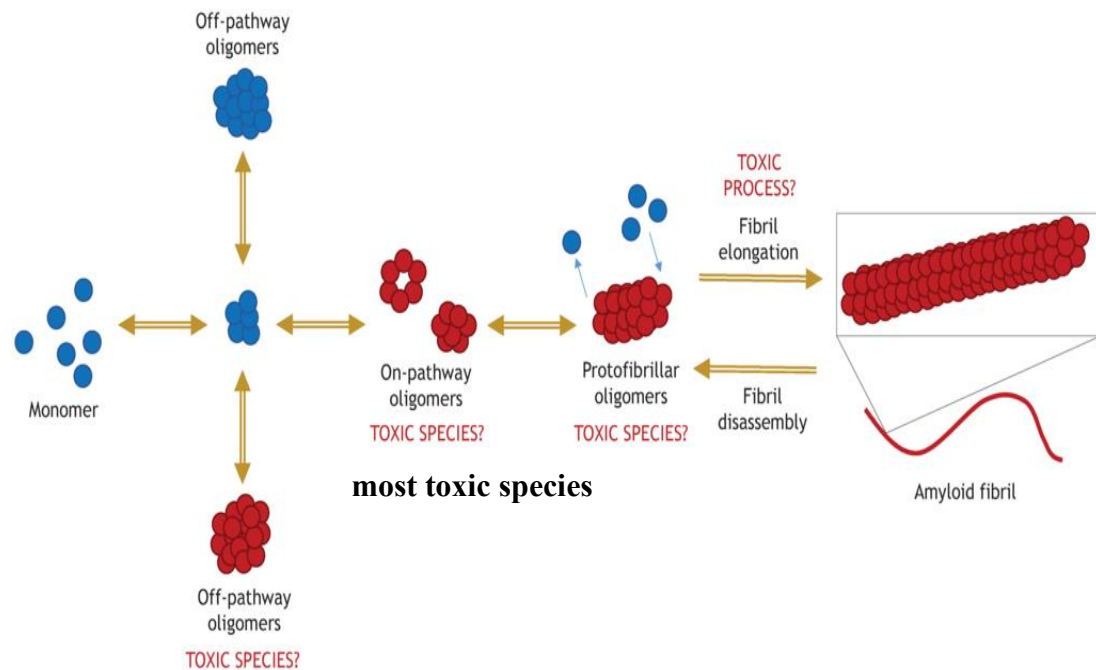


Figure 1.1 The process of amyloid fibril formation through oligomerization. Reproduced and adapted from Baldwin *et al.*, 2011, Licenced under CC BY 4.0.

PD ranks as the second most prevalent among neurodegenerative disorders, after AD. The disorder is characterized by distinct neuropathological alterations within the substantia nigra pars compacta of the midbrain, which encompass intracellular aggregates termed Lewy bodies (LBs). These LBs predominantly consist of α -syn. The diagnosis of PD relies on historical records and physical examinations of patients. The symptoms of the disease encompass both motor and non-motor manifestations. Motor symptoms encompass resting tremor, slowed gait movement, muscular rigidity, bradykinesia (slowed movement), and eventual imbalance. The amalgamation of these motor symptoms is referred to as Parkinsonism (Fu, 2018). The non-motor symptoms of PD often cause distress to patients and are broadly categorized into psychiatric, autonomic, sleep, and sensory symptoms. Among these, some of the most prevalent

symptoms comprise apathy (lack of interest and emotional engagement), constipation, disruptions in sleep patterns, hallucinations, and orthostatic hypotension (a drop in blood pressure upon standing). These symptoms are observed in approximately 60-70% of patients (Reich and Savitt, 2019). Additional non-motor symptoms encompass anhedonia (the inability to derive pleasure from previously enjoyable activities), diminished sense of smell and taste, excessive sweating, fatigue, and mood disturbances (Sveinbjornsdottir, 2016). Depression and anxiety have a higher likelihood of developing, particularly when the disease is inadequately managed or remains undiagnosed (Siuda, 2021).

The exact cause of PD is not thoroughly comprehended. However, the human tau protein exhibits a strong inclination to rapidly aggregate and create insoluble fibrillar structures within the brain. As a result, it is implicated in the pathogenesis of PD. (Lopes et al., 2022; Ryan et al., 2020), Additionally, POP, a highly expressed enzyme in the brain, has been linked to various pharmacological conditions, including the promotion of oligomer aggregation in PD (Rostami et al., 2020). Approximately 5-15% of PD cases are associated with genetic factors. The disease exhibits an escalated risk primarily among the elderly population, with gender representing a moderate risk factor (Lee and Gilbert, 2016). Moreover, environmental elements are connected to an increased susceptibility to the disease, particularly in regions where there is extensive use of pesticides like annonacin and neurodegenerative-inducing chemicals such as 1-methyl-4-phenyl-1,3,4,6-tetrahydropyridine (MPTP).

Presently, the treatment approach for PD revolves around replenishing dopamine levels (Reich and Savitt, 2019). Levodopa, also known as L-3,4-dihydroxyphenylalanine, is recognized as the most efficacious symptomatic medication for PD management. However, prolonged usage of levodopa can give rise

to motor complications, particularly motor fluctuations termed as 'wearing off' and 'on-off' states, along with dyskinesia (Reich and Savitt, 2019). Fig. 1.2 provides an overview of some of the common drugs employed to manage PD.

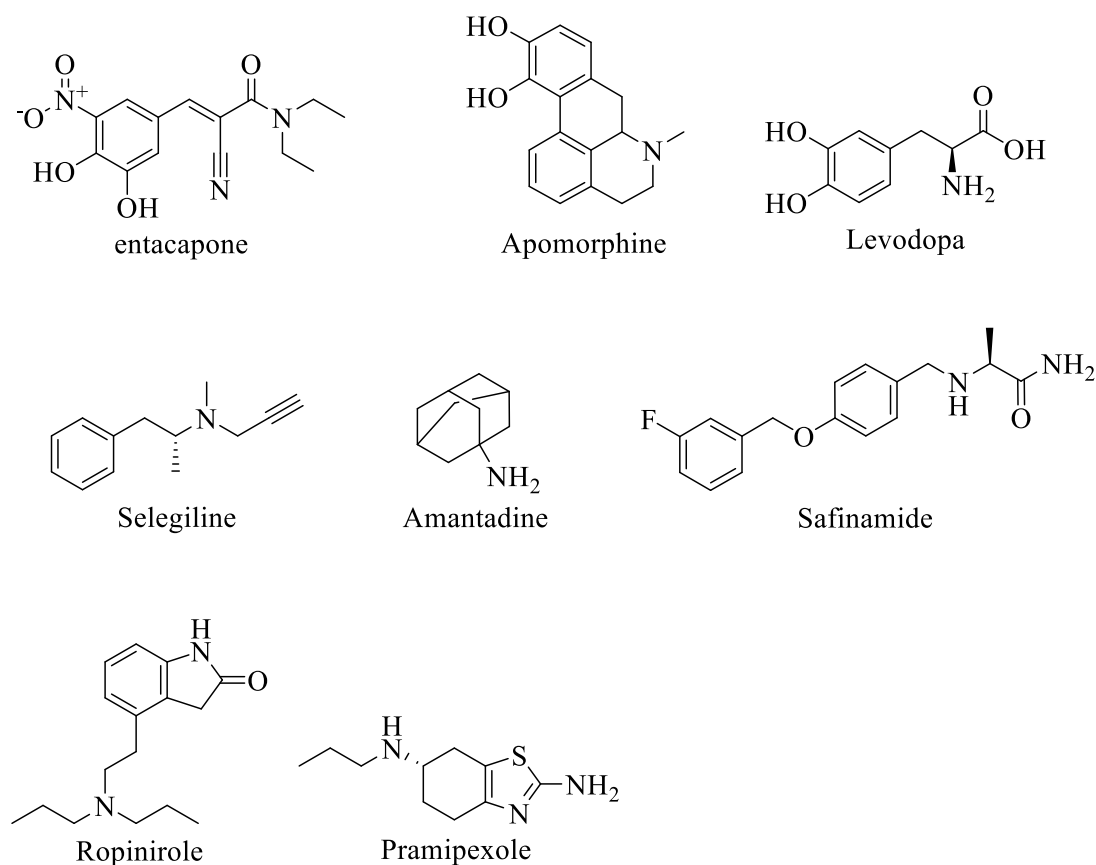


Figure 1.2 Compounds use to manage PD symptoms.

Natural products and herbal remedies have a rich history of traditional medicinal use and are gaining increased attention and popularity for treating various ailments. These remedies offer a wide array of chemical diversity, containing numerous compounds with diverse pharmacological activities. They are easily accessible, cost-effective, and generally have fewer side effects compared to synthetic alternatives (Hostalkova et al., 2019). However, despite their potential, natural products have received relatively little attention, and many plants and their constituents have been proposed as potential agents for enhancing cognitive behaviors and

addressing neurological conditions (Akter et al., 2021; Chen et al., 2021; Gregory et al., 2021; Hostalkova et al., 2019).

Yet, the process of discovering therapeutic drugs through experimental studies can be expensive, time-consuming, and resource-intensive. Moreover, these experiments might not always yield promising results (Balraadjsing et al., 2022; Nastaj and Wilczyński, 2021). In this context, computational approaches have gained prominence for validating potential compounds with optimized properties (Yadav and Eswari, 2023). Computational studies provide high-resolution insights and parameters that serve as valuable tools for screening large sets of potential therapeutic compounds. This approach reduces costs and eliminates candidates with unfavorable physicochemical properties, such as poor adsorption, distribution, metabolism, excretion, and toxicity (ADMET) characteristics, before subjecting them to further experimental evaluation (Lagorce et al., 2017; Yadav and Eswari, 2023).

1.2 Problem Statement

PD is characterized by the presence of abnormal aggregates in the brain, particularly involving α -syn, human tau, and toxic oligomers. Extensive evidence indicates that insoluble fibrils, notably those composed of α -syn, serve as the primary pathological hallmark of PD. The formation of α -syn begins with the aggregation of protein monomers into toxic oligomers, which further assemble into unstable protein protofibrils and eventually into insoluble fibrils, observed in PD. These toxic oligomers represent highly neurotoxic species implicated in the pathogenesis of PD (Koga et al., 2021). Moreover, the involvement of human tau protein and POP in PD pathogenesis is linked to increased aggregation of α -syn. These proteins contribute to disease progression and the development of pathological conditions. Prior research has

indicated the challenge in identifying compounds capable of preventing the formation of intracellular protein deposits, given the intricate nature of α -syn aggregation (Javed et al., 2019b; Karaki et al., 2022a). Many reported compounds primarily target α -syn as the main protein implicated in PD pathogenesis. Notably, a recent discovery, ASN90, acts as an inhibitor targeting two proteins (human tau and α -syn) (Permanne et al., 2022). However, several intracellular proteins, including α -syn, human tau, toxic oligomers, and POP, play roles in PD pathogenesis. As a result, there is a need for multi-target compounds capable of impeding disease progression by addressing two or more of these proteins, offering a potential therapeutic alternative. Hence, discovery of inhibitors targeting three key intracellular proteins (α -syn, human tau, and toxic oligomers) and one enzyme (POP). The ultimate goal was to identify potential alternative therapeutic candidates for PD treatment. This exploration was conducted using both computational *in silico* methods and *in vivo* zebrafish models, allowing for a comprehensive assessment of the compounds' potential efficacy and safety.

1.3 General Objective

The ultimate objective was to identify potential alternative therapeutic candidates for the treatment of PD.

1.4 Specific Objectives of the study

- i) To develop a ligand-based pharmacophore (LBP) models for α -syn and POP using selected inhibitors.
- ii) To perform virtual screening on natural (IBS) and semi-synthetic (Maybridge and Asinex) databases using the developed α -syn and POP pharmacophore models respectively.

- iii) To identify compounds that interact with at least three of the specified targets (α -syn, human tau, toxic oligomers, and POP) through docking analysis.
- iv) To evaluate the Absorption, Distribution, Metabolism, Excretion, Toxicity (ADMET) properties and stability of the selected compounds using MD *in silico* techniques.
- v) To assess the toxicity profile of the selected compounds using zebrafish embryo as an *in vivo* model.
- vi) To assess the inhibitory potential of the selected ligands through behavioral studies on a zebrafish animal model.

1.5 Flow chart of the research

The research flow of the study is depicted in Fig. 1.3, which summarizes into four categories: A, B, C, and D.

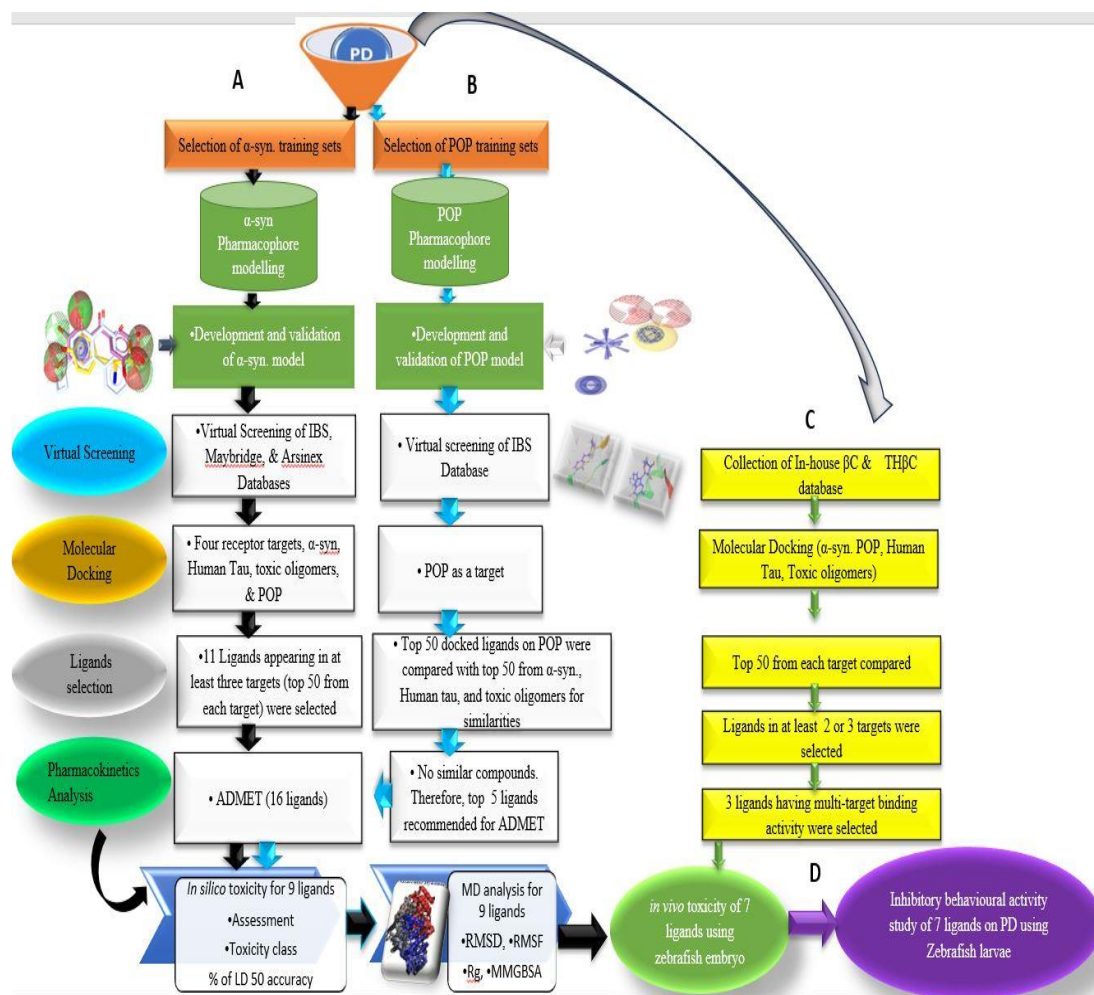


Figure 1.3 Summary of the research flow chart.

The research is divided into four stages (A, B, C, and D). Stages A and B entails the selection of α -syn and POP training sets, respectively, followed by the process of pharmacophore modelling, development, and validation process. The subsequent steps involve virtual screening of IBS, Maybridge, and Arsinex databases for model obtained from category A, while model obtained from category B is screened against IBS database only. Then the ligands retrieved from A category were docked onto the four essential targets (α -syn, toxic oligomers, human tau, and POP), while ligands obtained from category B were docked on POP only. Ligands appearing on at least three targets (A category) were considered multi-target compounds. The next stage involves subjecting the selected ligands to ADMET study, *in silico* toxicity, MD, *in vivo* toxicity and inhibitory behavioural study on PD using Zebrafish larvae (D). In stage C, the process involves the collection of in-house database compounds (derivatives of TH β C and β C from our laboratory), molecular docking onto the four essential targets, and selection of compounds appearing on at least two targets as multi-target ligands. The selected ligands from stage C were then subjected to ADMET screening, *in vivo* toxicity study, and inhibitor behavioural study using zebrafish larvae (D).

CHAPTER 2

LITERATURE REVIEW

2.1 Parkinson's Disease (PD)

PD was initially recognized over two centuries ago, in 1897, by Dr. James Parkinson (Jankovic and Tan, 2020). His milestone marked a major advancement in understanding the disease's pathological mechanisms. PD is a complex neurodegenerative disorder that primarily impacts dopaminergic neurons situated in a specific region of the brain known as the substantia nigra pars compacta. This leads to a reduction in dopamine levels and subsequent formation of abnormal intracellular inclusions called LBs (Permanne et al., 2022). The progression of PD's underlying pathological processes is gradual and involves multiple neuronal systems.

2.1.1 Symptoms of PD

The symptoms associated with PD are generally consistent across both adult males and females. However, numerous studies have indicated that these symptoms can differ among individuals due to the varied origins of the disease. Symptoms of PD are broadly categorized into two main groups: motor and non-motor symptoms (Lotankar et al., 2017; Reich and Savitt, 2019). The primary indicators used for diagnosing PD are its cardinal motor symptoms, which become apparent only as dopaminergic neurons sustain damage, resulting in a deficiency of dopamine in the substantia nigra pars compacta and subsequent symptom manifestation (Armstrong and Okun, 2020; Lotankar et al., 2017; Reich and Savitt, 2019). The progression of symptom manifestation is gradual, often making early identification challenging. Some of the motor symptoms include the following;

- (i) Tremor: There are various types of tremors, most commonly observed at rest, often described as a "pill-rolling" tremor due to the circular thumb-to-index finger movement. It may also be experienced during other activities. As PD advances, a loss of balance leading to falls can occur
- (ii) Muscle Rigidity: Particularly affecting the axial and limb regions, this refers to stiffness of the body.
- (iii) Postural Instability: This occurs when a patient struggles to maintain an erect posture, which can manifest at various stages of the disease
- (iv) Speech Disturbance: Many PD patients experience changes in speech characterized by soft, rapid talking. This is observed in more than half of PD cases
- (v) Bradykinesia: This signifies a difficulty initiating voluntary movements, with gradual reductions in movement speed and amplitude over time. It often leads to reduced facial expression (hypomimia) and smaller handwriting (micrographia) (Lotankar et al., 2017; Reich and Savitt, 2019).

Other motor symptoms encompass difficulties with swallowing, drooling of saliva, and dystonia, which is often associated with treatment and arises from abnormal movements and postures. Dystonia can result in unusual body positions and motions. Additionally, various postural deformities can emerge, such as camptocormia (abnormal forward flexion originating from the thoracic and lumbar spine) and antecollis (flexion of the head and neck) (Armstrong and Okun, 2020). Non-motor symptoms, on the other hand, may appear early on before a PD diagnosis is established, but their attribution to PD can be challenging. The diverse array of non-motor symptoms can lead to a delay in diagnosis due to potential overlap with other

pathological conditions (Armstrong and Okun, 2020). These non-motor symptoms are broadly classified into psychiatric, autonomic, sleep, and sensory categories.

Psychiatric symptoms encompass an inability to derive pleasure from once-enjoyable activities (anhedonia) and a lack of interest and emotional engagement (apathy). These symptoms, particularly anhedonia and apathy, often manifest prior to the commencement of treatment. Autonomic symptoms in PD include constipation, which occurs in approximately 60-70% of patients, as well as gastrointestinal issues, excessive sweating, fatigue, and mood disturbances (Sveinbjornsdottir, 2016).

Sleep plays a vital role in memory consolidation within the human body, particularly during slow-wave sleep. However, in the context of PD, sleep regulation becomes disrupted, leading to challenges like insomnia and excessive daytime sleepiness. Additionally, PD-related motor impairments often give rise to parasomnias, particularly rapid-eye-movement (REM) sleep disturbances. Other sleep-related issues encompass restless legs syndrome, inadequate muscle atonia, insomnia, sleep-related breathing disorders, circadian rhythm disruptions, daytime somnolence disorders, and sleep-related movement disorders (Elder et al., 2022; Lotankar et al., 2017). Sensory symptoms associated with PD include diminished smell and taste perception, visual impairments, olfactory disturbances, and pain. These symptoms often go unnoticed and are difficult for many clinicians to diagnose due to their elusive nature and the challenge of connecting them to PD. Furthermore, the improper management or diagnosis of PD may potentially lead to the development of depression and anxiety (Lotankar et al., 2017; Sveinbjornsdottir, 2016).

2.1.2 α -synuclein (α -syn)

The α -syn is a member of the group of proteins known as intrinsically disordered proteins (IDPs), found within LBs serving as a common link among various forms of Parkinsonism, including PD, variant PD, dementia with Lewi's body, and idiopathic PD. This protein's presence is considered a major pathological hallmark of PD, signifying damage to dopaminergic neurons, resultant dopamine depletion, and eventual development of PD (Jain et al., 2022; Schweighauser et al., 2022). The α -syn fulfill crucial roles in various biological processes, both within normal physiological functioning and in various chronic conditions such as PD (Meade et al., 2019). Human synucleins are categorized into three types: alpha (α), beta (β), and gamma (γ). These small, soluble proteins are primarily expressed in neurons, although they are also present in lower concentrations in other parts of the body. Notably, the α -syn molecule includes an amyloid-beta protein fragment, and sequence analysis of its amino acids (AA) has revealed an additional component referred to as the non-A-beta component (NAC). The precursor to NAC is known as NAC precursor (NACP) (Jain et al., 2022; Schweighauser et al., 2022).

The α -syn protein displays diverse forms, indicating its pathological diversity among synucleinopathies (Froula et al., 2019). While there is ongoing debate regarding whether α -syn exists in a dynamic equilibrium between unfolded monomers and α -helically folded tetramers under normal conditions, certain studies suggest that stable tetramers might indeed be one form of its existence (Alam et al., 2019). However, various reports have highlighted the presence of α -syn in dimers and trimers, particularly in diseases without reported mutations. This complexity poses challenges in targeting the α -syn protein with bioactive compounds (Glajch et al., 2021; Kumara et al., 2020; Melki, 2018). Due to its intricate nature, α -syn. holds an important interest

owing to its clinical relevance in the pathogenesis of PD (Acosta et al., 2019; Gilmozzi et al., 2020; Papagiannakis et al., 2018).

2.1.2(a) α -syn's structural characteristics

The α -syn is a compact protein composed of one hundred and forty (140) amino acid (AA) residues (Fig. 2.1), and its aggregation is closely associated with the pathogenesis and advancement of PD (Gómez-Benito et al., 2020). Its structural makeup comprises three primary domains:

- a. N-Terminal Domain: This segment, also referred to as the amino-terminal domain, is responsible for the formation of amphipathic helices. It encompasses eleven AA imperfect repeats, featuring a consensus motif denoted as KTKEGV.
- b. Central Hydrophobic Domain (NAC): This domain, positioned at the protein's core, is hydrophobic in nature and plays a pivotal role in fostering increased fibril formation
- c. C-Terminal Domain: The C-terminal domain, predominantly unfolded in nature, contains a high density of negatively charged AA residues (Gómez-Benito et al., 2020; Schweighauser et al., 2022; Yedlapudi et al., 2016).

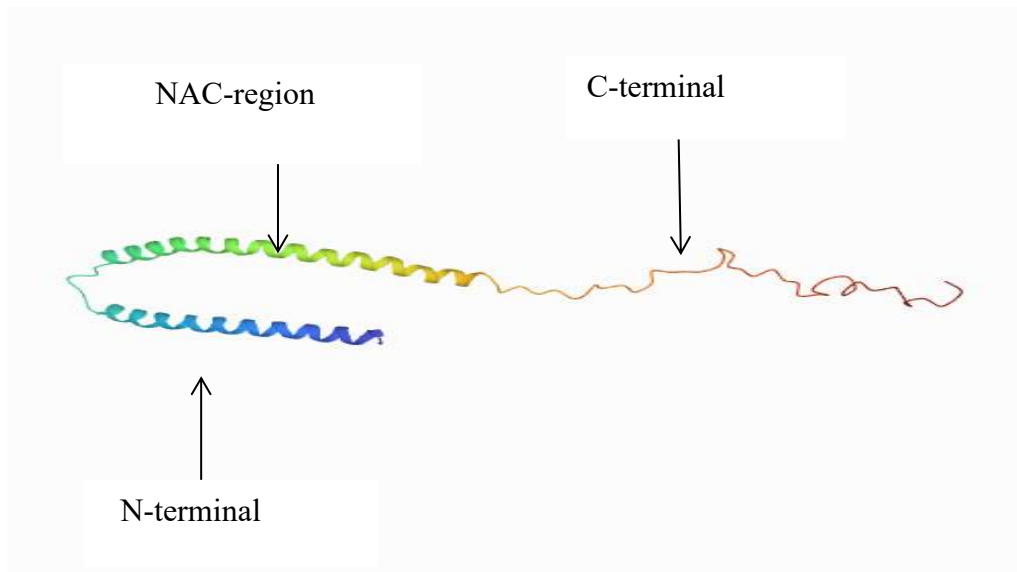


Figure 2.1 Structure of human micelle-bound α -syn retrieved from protein data Bank demonstrating its various domain.

At the amino acid (AA) sequence level (as depicted in Fig. 2.2), α -syn consists of three distinct AA regions:

- a. N-terminal (Residues 1–60): This segment is characterized by amphipathic α -helices, spanning residues 1 to 60.
- b. Non Amyloidogenic component (NAC) Region (Residues 61–95): Encompassing residues 61 to 95, this hydrophobic region is notably amyloidogenic and contributes to fibril formation.
- c. C-Terminal Region (Residues 96–140): The third region, comprising residues 96 to 140, is rich in highly acidic amino acids.

The initial two regions collectively form a membrane-binding domain, while the C-terminal tail encompasses sites for protein-protein and protein-small molecule interactions (Gómez-Benito et al., 2020).

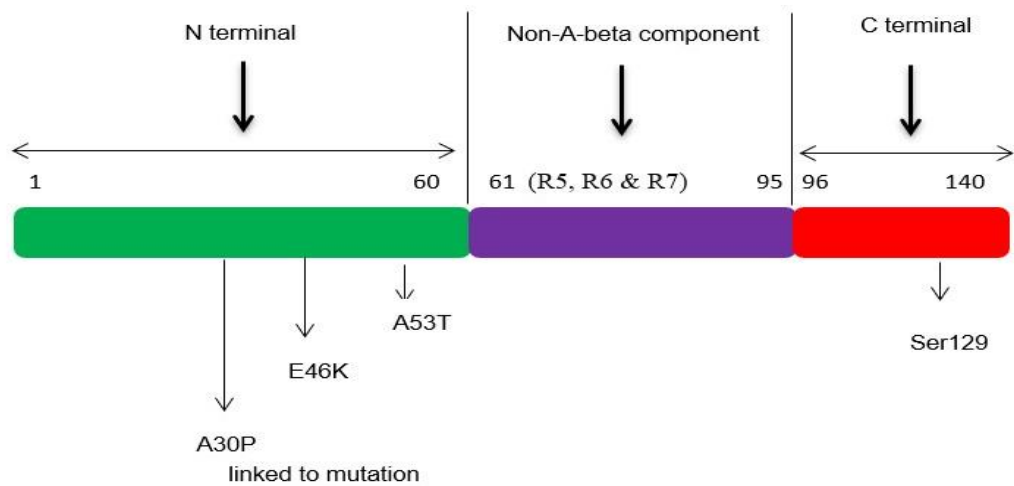


Figure 2.2 Structure of α -syn showing the NAC domain.

The N-terminal domain of α -syn has been identified to contain six specific point mutations: A30P, E46K, A53T, A53E, H50Q, and G51D. Notably, among these mutations, A30P, E46K, and A53T are the most prevalent as illustrated in Fig. 2.2 above. These mutations are associated with autosomal dominant forms of PD, underscoring their clinical relevance as potential therapeutic targets (Schweighauser et al., 2022). These three mutations A30P, E46K, and A53T exhibit a propensity to accelerate fibril formation compared to the native α -syn structure. In a murine model, the expression of human A53T α -syn has been observed to disrupt dopamine transport. The A30P mutant variant of α -syn appears to impact the binding of the cell membrane to lipids, while the E46K mutation results in an increased aggregation tendency and may consequently affect its normal function (Ayipo et al., 2020; Schweighauser et al., 2022). These findings highlight the potential significance of modulating these mutations as a therapeutic avenue for PD treatment.

2.1.2(b) Role and function of α -syn

The α -syn serves as a highly abundant, soluble protein primarily found in nerve terminals, and it assumes a central role in the pathogenesis of PD. Its functions are multifaceted and crucial to the proper functioning of neuronal processes. One of its pivotal roles involves the regulation of synaptic vesicle recycling, vesicular storage, and the release of neurotransmitters, contributing to synaptic activity (Sorrentino et al., 2021). Previous investigations have indicated that α -syn also participates in the modulation of various neurochemical processes. It is implicated in the regulation of the enzyme tyrosine hydroxylase, which is integral to dopamine synthesis, as well as in the modulation of dopamine transporter activity and the regulation of monoamine transporters (Román-Vendrell et al., 2021). These multifaceted functions are summarized in Fig. 2.3. Interestingly, certain studies have highlighted that an overexpression of α -syn, mutations in the protein, and dopamine-modified α -syn can promote detrimental interactions between its oligomers and lipid structures (Itokazu et al., 2021; Snead and Eliezer, 2014; Yedlapudi et al., 2016). This subsequently leads to the aggregation, propagation, phosphorylation, and misfolding of the protein, all of which have been implicated in the underlying mechanisms of PD onset and development (Alza et al., 2019; Schweighauser et al., 2022).

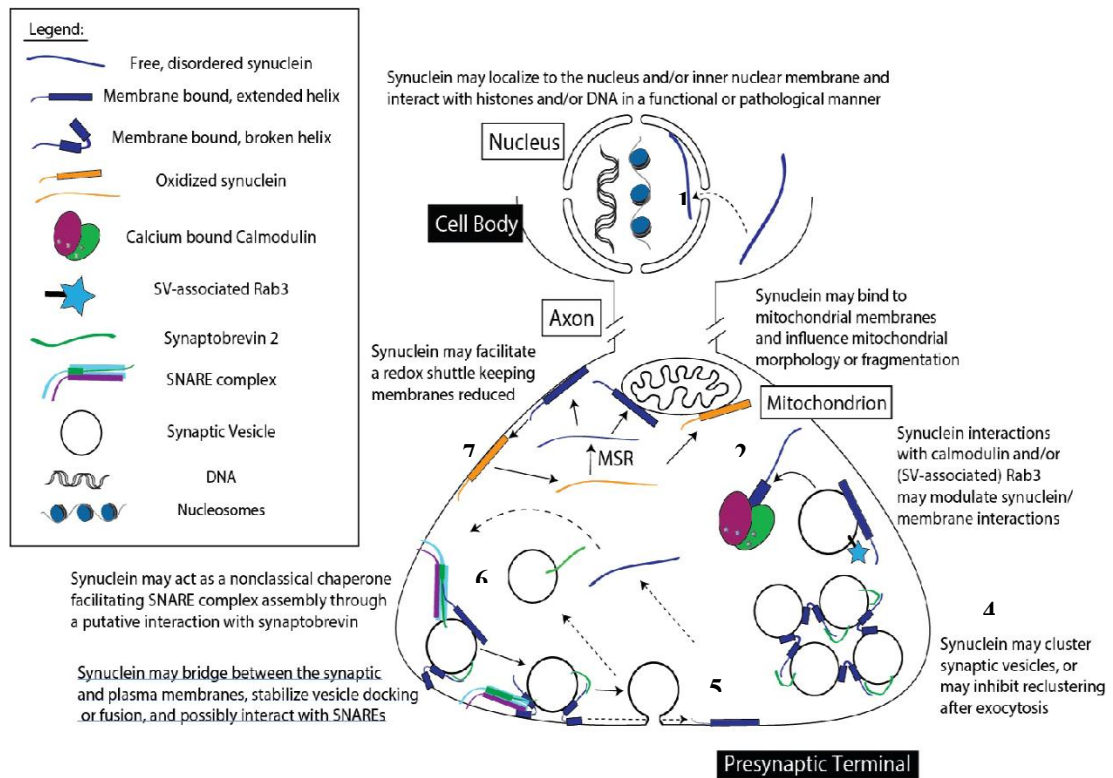


Figure 2.3 Functions of α -syn and its role in disease state. Reproduced and adapted from Snead and Eliezer 2014, Licenced under CC BY 4.0.

1, The disordered α -syn can localize to the nucleus or inner membrane, potentially engaging with DNA or histones. This interaction may have both functional and pathological implications. 2, the α -syn binds to the mitochondrial membrane, where oxidized forms of α -syn extend into a helical structure. Some oxidized α -syn molecules also bind to neuronal walls, affecting their morphology and fragmentation. 3. Interaction with calmodulin allows α -syn to moderate membrane interactions. 4, At presynaptic terminals, α -syn clusters vesicles and inhibits their re-clustering after exocytosis, influencing cellular processes. 5, It serves as a bridge between the plasma and synaptic membranes, contributing to the stabilization of vesicle docking and fusion. 6, α -syn acts as a nonclassical chaperone, aiding in the assembly of SNARE complexes. This interaction, particularly with synaptobrevin, facilitates membrane fusion and the exocytosis of neurotransmitters, thereby maintaining effective signal transmission at synapses. 7, Additionally, α -syn participates in a redox shuttle, contributing to the reduction of membranes.

These diverse roles highlight the multifunctionality of α -syn and its important involvement in various cellular processes, which can have both physiological and

pathological consequences in understanding PD and developing therapeutic strategies to mitigate the impact of α -syn-related neurodegenerative diseases.

2.1.2(c) Structural alterations of α -syn

The structural modifications of α -syn that contribute to the pathogenesis of PD development involve various neurodegenerative mechanisms, including aggregation, propagation, misfolding, and phosphorylation (Mukhopadhyay et al., 2019).

2.1.2(c)(i) Aggregation and propagation

The aggregation of α -syn within LBs primarily occurs through its natural binding to the cell membrane. Monomeric α -syn binds to the membrane and adopts an α -helical conformation, leading to the formation of membrane-bound β -sheets (Mehra et al., 2019). Cholesterol and lipids also play a major role in α -syn aggregation (Mukhopadhyay et al., 2019). The self-association of oligomers results in the formation of membrane-bound β -sheet structures that mediate α -syn toxicity. Experimental models have demonstrated that α -syn aggregates form under conditions of elevated protein concentration, extended incubation time, a temperature of 37°C, and the presence of specific metal ions, as well as the addition of dopamine (García-Sanz et al., 2020).

Research has indicated that α -syn can spread through a cell-to-cell transmission mechanism. Monomeric and oligomeric forms of the protein are present in both human neurons and cell cultures, and this cell-to-cell transmission has been observed in human and animal PD models (Rodrigues et al., 2022). This phenomenon has led to the "prion-like" hypothesis, suggesting that α -syn is transmitted between cells via the extracellular space, leading to protein misfolding (Oertel and Schulz, 2016). It is

proposed that the misfolding of α -syn begins in the recipient cell, giving rise to LBs. The conditions promoting α -syn misfolding result in an increased level of the protein outside the cells. Consequently, an excess of α -syn released from the cell induces neurotoxicity in nearby cytoplasm, causing damage within the extracellular space (Najib et al., 2022; Strang et al., 2019).

2.1.2(c)(ii) Misfolding of α -syn

The processes underlying the misfolding of α -syn leading to the formation of fibrils and subsequently to LBs, remain poorly understood (Dehay et al., 2016). A study by Mahul-Millier et al. (2020) has proposed that the aggregation of α -syn outside LBs and Lewy neurites (LNs) is hypothetically much more important than that occurring within these structures. This heightened aggregation and misfolding of α -syn may contribute to synaptic dysfunction and neuronal cell death (Mahul-Mellier et al., 2020). Recent research has demonstrated that the introduction of preformed fibrils (PFFs) can initiate misfolding and aggregation of α -syn, as illustrated in Fig. 2.4 A and B, both in cell cultures and animal models of PD (Rodrigues et al., 2022). Furthermore, earlier findings suggest that an excess of α -syn, along with its mutations, can facilitate toxic interactions between α -syn oligomers and the cell membrane lipids (Sorrentino et al., 2020).

2.1.2(c)(iii) Phosphorylation and toxicity of α -syn

Post-translational modifications (PTMs) of α -syn, such as phosphorylation, ubiquitination, cross-linking, protein chain truncations, and nitration, are commonly reported. These variations in PTMs play a crucial role in regulating the accumulation and toxicity of α -syn (Rondón-Villarreal and López, 2020). Phosphorylation involves

the reversible addition of a phosphate group (PO₄) to the polar group R of amino acids, catalyzed by protein kinases (Kawahata et al., 2022). Notably, phosphorylation of α -syn at the serine residue (S129) has garnered important interest due to its substantial implication in neurodegeneration and neurotoxicity. This modification is particularly relevant for the interaction between the protein and lipid molecules on the surface of the mitochondrial cell membrane (Ardito et al., 2017; Kawahata et al., 2022; Reynolds et al., 2011). Numerous studies have demonstrated the phosphorylation of α -syn using various experimental models, including *in vitro* cell cultures, *in vivo* zebrafish, *Maurine*, and fruit flies (Reynolds et al., 2011; Rondón-Villarreal and López, 2020; Schweighauser et al., 2022; Török et al., 2016). This phosphorylation event contributes to our understanding of the protein's role in neurodegenerative processes and its potential as a therapeutic target.

A previous study indicated that inhibiting the ubiquitin-proteasome system and the autophagy-lysosomal pathway led to a notable increase in phosphorylated α -syn in neuroblastoma, suggesting that phosphorylation could play a role in α -syn degradation (Peng et al., 2018). However, there is an ongoing debate about the active role of phosphorylation in the accumulation and toxic effects of α -syn (Ghanem et al., 2022). A study by Gilmozzi *et al.* (2020) strongly supports the hypothesis that phosphorylation at S129 plays a crucial role in regulating α -syn's normal functions, controlling its aggregation, fibrillation, LBs formation, and neurotoxicity (Gilmozzi et al., 2020).

Beyond aggregation, propagation, misfolding, and phosphorylation, other proteins such as oligomers, human tau, and POP also contribute to the pathogenesis of NDs, particularly PD, through mechanisms related to α -syn modifications (Najib et al.,

2022; Oueslati, 2016). Investigating these interactions further could provide valuable insights into the complex network of processes underlying neurodegeneration in PD.

2.1.2(d) Therapeutic alternatives inhibitory compounds of α -syn

In the pursuit of therapeutic alternatives, inhibitory compounds targeting α -syn have garnered an important attention as a critical strategy to combat synucleinopathies. The selection of α -syn inhibitors should be meticulous, focusing on their capacity to effectively target the toxic species of the protein, potentially leading to the development of potent inhibitors capable of transforming toxic oligomers into non-toxic forms (Tanaka et al., 2019).

Numerous candidates have been explored in both *in vitro* and *in vivo* studies, specifically aiming at different components of the α -syn fibrillization pathway, particularly its fibril forms (Mehra et al., 2019; Vaikath et al., 2019). In a study by Chatterjee et al. (2018), nanobodies such as H14PEST and NbSyn87PEST which are small size single-domain antibodies derived from the immune system of certain species of camelids were found to target a specific pathogenic pathway, particularly the non-amyloid component and the C-terminal region of α -syn fibrils. This targeting resulted in a major reduction in S-129 phosphorylation, as observed in an *in vivo* Sprague–Dawley rat model (Chatterjee et al., 2018). Nanobodies exhibit promising potential for PD treatment, although challenges related to production difficulty and potential immune reactions need to be addressed.

Recent attention has also been directed towards both natural and synthetic small molecule compounds that exhibit potential inhibitory effects on α -syn fibrils (Chatterjee et al., 2018). Of note are unsubstituted phenothiazine (PTZ) scaffolds, which serve as parent molecules for numerous drugs and their derivatives (Fig. 2.4).

PTZ compounds have attracted major interest due to their intrinsic properties, such as high lipophilicity, ability to readily cross the blood-brain barrier (BBB), strong antioxidant effects that mitigate neuronal damage, and low susceptibility to toxicity, central nervous system depression, and carcinogenicity (Najib et al., 2022; Wegrzynowicz et al., 2019). However, it is important to note that these compounds have shown limited success in curing or reversing PD, mainly due to their single-target inhibitory approach against α -syn protein. Further research is warranted to develop multi-target compounds that address the complex pathomechanisms underlying PD development.

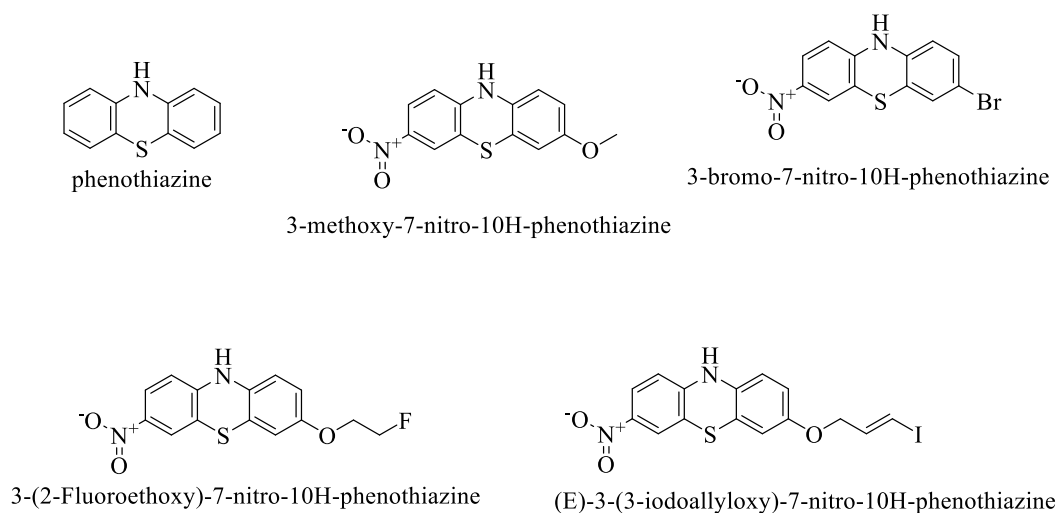


Figure 2.4 Chemical structure of phenothiazine and its derivatives

PTZ derivatives that have demonstrated potential anti-PD properties by binding to α -syn fibrils include 3-methoxy-7-nitro-10H-phenothiazine, 3-Bromo-7-nitro-10H-phenothiazine, 3-(2-Fluoroethoxy)-7-nitro-10H-phenothiazine, and (E)-3-(3-Iodoallyloxy)-7-nitro-10H-phenothiazine (Tapias et al., 2019). These derivatives exhibit affinity for α -syn fibrils and have been investigated for their therapeutic potential in PD. However, despite their promising attributes, the development of extrapyramidal side effects (such as acute dystonia, akathisia, and dyskinesia) and

anticholinergic side effects (including dry mouth, constipation, tachycardia, and sedation) has been observed with these compounds. However, it is important to note that these compounds have shown limited success in curing or reversing PD, mainly due to their single-target inhibitory approach against α -syn protein. Further research is warranted to develop multi-target compounds that address the complex pathomechanisms underlying PD development (Javed et al., 2019a; Najib et al., 2022).

Polyphenolic compounds derived from natural plants have emerged as promising alternative ligands for the management of NDs (Singh et al., 2020). These polyphenols are naturally occurring compounds abundant in various plant sources and have been associated with a wide range of pharmacological activities, including neuroprotection (Lee et al., 2020; Najib et al., 2022). Among the diverse array of bioactive plant compounds, flavonoids are among the most extensively studied. Flavonoids are a type of polyphenol found in fruits, vegetables, and plant-based beverages, known for their antioxidant, antimutagenic, and antiproliferative properties (Ghasemi Tigan et al., 2019). These attributes suggest that flavonoids may have a protective role in mitigating the development of NDs (Nagula and Wairkar, 2019).

Prominent among the alternative ligands derived from plant natural compounds targeting α -syn aggregation is anle138b, an oligomer modulator. This compound has been reported to inhibit α -syn protein aggregation, leading to restored dopamine release, prevention of cell death, and improved gait impairment in a transgenic mouse model (Chatterjee et al., 2018). In a similar vein, other studies have highlighted the potential of compounds such as crocin and baicalein and its analogue (Fig. 2.5) as effective inhibitors of α -syn fibril formation.